Proceedings of the ASME 2022 41th International Conference on Ocean, Offshore and Arctic Engineering
OMAE2022-79673
June 5-June 10, 2022, Hamburg, Germany

OMAE2022

A PHYSICAL-BASED DAMPING MODEL OF GAP AND MOONPOOL RESONANCE IN WAMIT

Senthuran Ravinthrakumar
SINTEF Ocean
Dept. of Marine Operations
Trondheim, Norway
Email: senthuran.ravinthrakumar@sintef.no

Babak Ommani
SINTEF Ocean
Dept. of Energy
Trondheim, Norway

Trygve Kristiansen
NTNU
Dept. of Marine Technology
Trondheim, Norway

Idunn Olimb
Equinor
Dept. of Offshore Wind Competence
Bergen, Norway

Bernt Karsten Lyngvær
Equinor
Dept. of Offshore Wind Competence
Bergen, Norway

ABSTRACT

An engineering model to estimate and incorporate quadratic damping of the piston-mode moonpool responses in the proximity of the piston mode period is proposed. The model provides a physical-based equivalent linearized damping coefficient. The method is not limited to forced motion, but applicable to freely floating moonpool vessels. Further, it is not limited to moonopools, but can be generalized to gap resonance problems, such as side-by-side operations. The soundness of the proposed physical-based method is demonstrated using the panel code WAMIT with a linear damping term in the free-surface boundary condition inside the moonpool using two existing moonpool experiments as case studies; (1) a two-dimensional rectangular box with a moonpool subject to forced heave, and (2) a freely floating offshore vessel in incident waves. The WAMIT computations using the proposed method reconstructs the experimentally obtained piston-mode and vessel responses well. We suggest that the proposed method can be used with fair degree of confidence in an early design or operational analysis phase, in the (often) case that the quadratic damping is not known from either experiments or CFD. To our knowledge, this is the first general, physical-based piston-mode damping model that does not require any tuning from experiments.

NOMENCLATURE

B Beam of vessel mid-ships.
ε Fluid damping coefficient.
ε_m Fluid damping coefficient for moonpools.
η_{ia} Motion amplitude in i-direction.
D Draft.
FDS Fluid damping surface.
ω Circular frequency.
g Gravitational constant.
H Incident wave height.
K Pressure drop coefficient.
κ Scale factor.
L Length of vessel.

L_g Gap length.
λ Wavelength.
m Dry mass of vessel.
p Pressure.
ϕ Velocity potential.
RAO Response amplitude operator.
ρ Density of water.
Sn Solidity ratio.
t Time.
T Wave period or forced oscillation period.
T_0 Piston mode period.
WP Wave probe.
ζ_a Incident wave amplitude.
ζ_g Gap response amplitude.
ζ_{mp} Moonpool response amplitude.

INTRODUCTION

A moonpool is a vertical opening in a ship structure. It is well known that one might experience significant resonant piston-mode motions; the oscillations can reach several times that of the incident wave height. Resonant moonpool motions can be associated with large waiting time, which affects the operability of a moonpool vessel.

It is therefore of great engineering interest both in vessel design and in planning of marine operations to have a rational damping model at hand, to be used in state-of-the art tools such as linear potential flow theory based panel codes.

Without additional damping, it is well known that panel codes greatly over-predict both the piston-mode and vessel responses to such an extent that the simulations are rendered unphysical. The reason is that only potential flow wave radiation damping is included, while the dominant source of damping is that due to flow separation at the moonpool inlet. Kristiansen and Faltinsen (2008) [1] showed that, at least in traditional size moonpools, the quadratic type damping due to flow separation at the moonpool inlet is the dominant source of damping for the piston-mode using a BEM + vortex tracking method.

Prior and also after this discovery, many people have used various variations of including additional, artifical damping in panel codes. Some quite recent examples are [2] and [3]. See also the papers cited therein. Common to many of these studies is that the (artificial) damping parameter is tuned to experiments to which the numerical simulations are compared with. This means that, despite significant and good efforts in producing efficient and novel numerical or semi-analytic solutions as in the references above, the computations suffer from that the results are unphysical without the input from either experiments or CFD simulations of the moonpool vessel at hand.

In the present study, we propose a physical-based model to estimate the quadratic damping due to flow separation at the moonpool inlet, whithout the use of tuning to model tests or CFD simulations. The model is based on the novel idea suggested by Faltinsen and Timokha (2015) [4]. Their model is based on existing pressure loss coefficients for slatted screens in the literature, as well as the moonpool vessel geometry. It was inspired by the understanding that flow separation at the moonpool inlet is the main source of piston-mode damping.

A version of the method was implemented by Ravinthrakumar (2020) [5] in a 2D time-domain BEM, where promising results were given in the application of moonpool resonance. In the present paper, we further develop the model.

We exemplify the validity of the proposed damping model in two case studies; one for a simplified 2D moonpool vessel forced to heave, and one for a freely floating vessel exposed to incident head-sea waves. We express the quadratic damping term by means of equivalent linearized damping, and apply the linear panel code WAMIT with a linear damping term included in the free-surface condition inside the moonpool.

The physical-based damping model can be generalized to gap resonance problems, such as side-by-side operations.

MODEL TESTS

We here give an overview of the two sets of model tests that we use as validation data for our proposed damping model. We refer to these as Case 1 and 2. Both tests have previously been carried out, but they are briefly described here for completeness of the present text.

Case 1. Forced heave of a 2D moonpool vessel

The first case involves forced heave of a body consisting of two rigidly connected rectangular boxes in a two-dimensional setting, as sketched in Figure 1. The tests are described in [7], but main particulars are given in the following.

The tests were carried out in a narrow wave flume with breadth 0.60 m. The breadth of the model was 0.595 m, i.e. nearly fitting within the wave flume width. Referring to Figure 1,

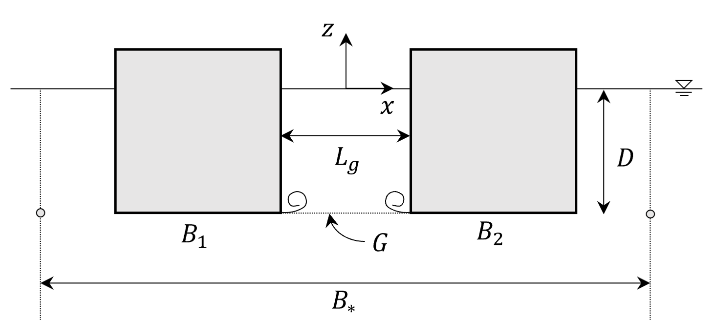

FIGURE 1. SKETCH ILLUSTRATING A 2D MOONPOOL. THE SOURCES AND B_* AS DEFINED BY MOLIN (2001) [6] ARE INDICATED BY THE CIRCLES.

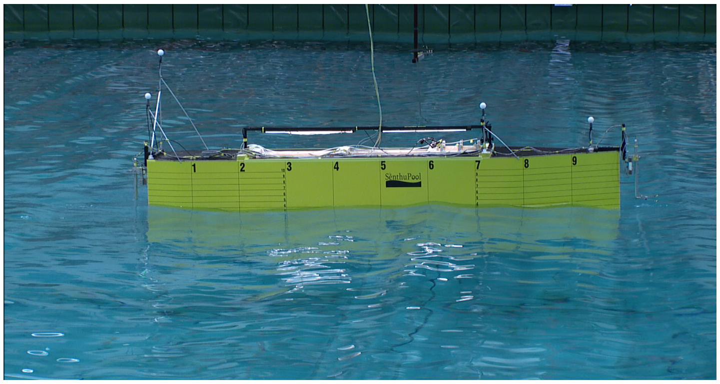

FIGURE 2. EXPERIMENTAL SET-UP IN THE OCEAN BASIN AT SINTEF OCEAN, WHERE A SHIP WITH MOONPOOL IS FREELY FLOATING. THE MODEL IS 4 m LONG, THE MID-SHIP BEAM IS 0.8 m, AND THE TOTAL HEIGHT IS 0.6 m. THE DRAFT DURING THE MODEL TESTS WAS 0.2 m.

dimensions were: $D = 0.18$ m, $B_1 = B_2 = 0.36$ m and $L_g = 0.18$ m. The model was forced to heave sinusoidally with a range of forcing frequencies around the piston-mode natural period, and with two heave amplitudes, $\eta_{3a} = 0.0025$ m and 0.005 m. The free-surface elevation was measured by two wave probes, and the piston-mode amplitude ζ_g was taken as the mean of these. The free-surface was observed to be nearly flat inside the moonpool, i.e. dominated by the piston-mode. Both signals were band-pass filtered around the forcing frequency, and steady-state amplitudes, denoted by $\zeta_g^{(\omega)}$ and $\eta_{3a}^{(\omega)}$, were extracted from a steady time-window. The (amplitude-dependent) moonpool RAO was taken as the ratio $\zeta_g^{(\omega)}/\eta_{3a}^{(\omega)}$.

Case 2. Freely floating moonpool vessel

The second of our two validation cases involves a freely floating moonpool vessel. Experimental studies were carried out in the Ocean Basin at Sintef Ocean in Trondheim, Norway, as described in [5]. The main particulars and set-up are provided herein for completeness of the text. The basin is 80 m long, 50 m wide and the water depth was 5 m. Vessel and moonpool responses were studied in long-crested waves.

The model length was 4 m, and a scale of 1:34.5 was imagined. Other main particulars of the ship model are summarized in Table 1. A photo of the model is presented in Figure 2. The hull has vertical walls and horizontal bottom. The model is not equipped with bilge keels, but has sharp-edged bilges.

The experiments were carried out with the model freely floating in incident waves. Irregular and regular wave tests were conducted, and we use results from regular waves with two different wave steepnesses $H/\lambda = 1/30$ and $1/60$ here. The duration of the regular wave tests was three minutes, with a waiting time of six minutes between each test for the basin to calm down.

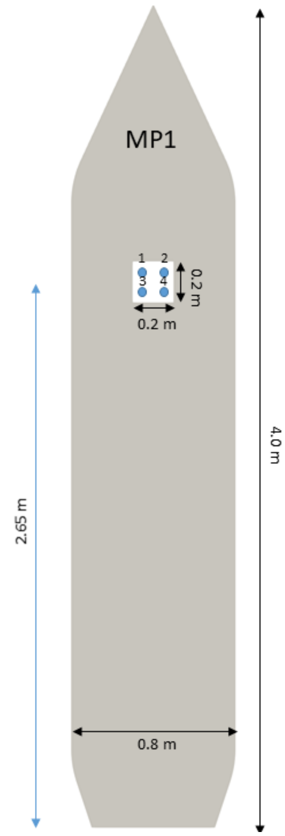

FIGURE 3. BIRD'S EYE VIEW OF THE WAVE PROBES IN THE MOONPOOL. THE MODEL DIMENSIONS ARE INDICATED. THE DISTANCE FROM THE AFT TO THE CENTRE OF THE MOONPOOL IS INDICATED. THE WAVE PROBES ARE PAIRWISE DISTRIBUTED IN THE MOONPOOL, WITH A DISTANCE OF 5 cm FROM THE MOONPOOL WALLS.

Results from a steady-state time-window are presented in this paper.

The vessel was moored with four horizontal mooring lines, each with a stiffness of 90 N/m. The pre-tension in the mooring line was prescribed to be 45 N.

Three different moonpool sizes were tested, referred to as MP1, MP2 and MP3 (cf. Ravinthrakumar et al. (2020) [8]), where MP1 represents a conventional moonpool size, is used here.

Cradle tests were conducted to determine the radius of gyration in pitch and center of mass of the naked and fully equipped models with added weights. The total mass was also measured during this process. The results were compared to calculations using the CAD software Rhino, and differences less than 0.5 % were obtained.

The model was equipped with four body-fixed wave probes (WPs) evenly and pairwise distributed in the moonpool, as illus-

TABLE 1. MAIN PROPERTIES OF THE PRESENT SHIP MODEL. A SCALE OF 1:34.5 IS IMAGINED. THE MOONPOOL CENTER IS MEASURED RELATIVE TO THE ORIGIN OF THE COORDINATE SYSTEM.

Parameter	Model scale
Length (L)	4.0 m
Beam (B)	0.8 m
Draft (D)	0.2 m
Moonpool length (L_m)	0.2 m
Moonpool width (B_m)	0.2 m
Moonpool center ((c_x, c_y, c_z))	(0.65 m, 0 m, 0 m)
Ship mass (m)	526.7 kg
Center of gravity (COG)	(-0.11 m, 0 m, 0.055 m)
Radius of gyration ((r_x, r_y, r_z))	(0.28 m, 1.02 m, 0.76 m)

trated in Figure 3. In addition, six Earth-fixed wave probes were used outside the model. Oqus position system was used to measure the motion in six directions. The model was equipped with three body-fixed accelerometers, each measuring accelerations in x-, y- and z- directions.

Several repetition tests were conducted during the model test campaign. Selected waves were repeated eight times for a given wave period and wave steepness. The standard deviation in the repetition tests was less than 1 % relative to the mean value, in general. Several video recordings and photos were taken during the model tests, which served as a tool to interpret the model test results. Selected video recordings are presented by Ravinthrakumar et al. (2020) [8].

PHYSICAL-BASED MOONPOOL DAMPING MODEL

We now present the physical-based moonpool piston-mode damping model.

The industry standard panel code WAMIT is used to perform the present numerical simulations. WAMIT introduced the possibility of introducing linear damping to damp resonant fluid motions. A linear damping term, proportional to the vertical water velocity, w, is introduced in the linearized dynamic free-surface condition as

$$\frac{p}{\rho} = -i\omega\phi - g\zeta = \varepsilon\frac{\partial\phi}{\partial z}, \qquad (1)$$

where p is the pressure, ρ is the density of water, ϕ is the velocity potential, g is the gravitational acceleration, ω is the circular frequency, and ζ is the free-surface elevation. This condition expresses that there is a jump in pressure from the atmospheric to that in the water at the free surface. Since the pressure jump is proportional to the vertical water velocity, it acts as a damping thinking in terms of the piston-mode as a near rigid-body mode.

The damping is implemented in WAMIT by defining panels on the free-surface in the moonpool (or gap). In this paper, we refer to these panels as fluid damping surfaces (FDS).

The problem now lies in developing a physical-based expression for ε. We suggest to use the method proposed by Faltinsen and Timokha (2015) [4]. A version of the method was implemented by Ravinthrakumar (2020) [5] who showed promising results in the application of moonpool resonance.

Briefly summarized, the physical domain $z \leq 0$ is mirrored to the upper half plane $z > 0$. Next, the body is mirrored repeatedly also through two imagined vertical surfaces, one on each side of the body, such that the final geometry consists of infinitely many bodies, resembling a slatted screen submerged in infinite fluid. The resulting flow then resembles the flow around a slatted screen in infinite fluid. This can be used to estimate the drop in pressure based on published results from experiments of slatted screens subjected to oscillatory flow. The pressure drop for a slatted screen in infinite fluid is assumed to be quadratic with respect to the ambient velocity,

$$\Delta p = \frac{1}{2}\rho K|w|w, \qquad (2)$$

where $w = \partial\phi/\partial z$ is the ambient fluid velocity, ρ is the density of the fluid and K is the pressure drop coefficient.

There are two consequences of the fact that we have a free surface, and not infinite fluid. One is that the pressure drop for our moonpool problem is only half that for a slatted screen in infinite fluid, as argued by [4], due to that the flow separation only occurs at the lower side of the screen (the moonpool inlet). We therefore denote the pressure drop in the moonpool by $\Delta p_g = 0.5\Delta p$. More specifically, Δp_g is the drop in pressure over the moonpool entrance, denoted by G in Figure 1.

Secondly, the ambient fluid velocity w is not given in our moonpool problem, as it is in oscillatory, uniform flow in infinite fluid. [4] suggested to relate the ambient velocity w to that of the piston-mode, called W, by a mass-conservation argument. They re-write (2) as

$$\Delta p_g = \frac{1}{4\gamma^2}\rho K|W|W, \qquad (3)$$

where $W = w\gamma$ is the vertical fluid velocity at the free-surface, and $\gamma = B_*/L_g$. The variables B_* and L_g are schematically presented in Figure 1, and B_* is treated further below. The fraction

γ represents an efficient solidity ratio, where solidity ratio means solid area relative to the total area of the screen.

To proceed, we express the quadratic damping due to the pressure drop by means of an equivalent linearized damping coefficient. This involves as usual equating the amount of work that the linear pressure drop in (1) performs on the moonpool free surface, to the work that the quadratic pressure drop (3) performs on the imagined surface covering the moonpool inlet, i.e.

$$\int_0^T \varepsilon W W dt = 4 \int_0^{T/4} \frac{1}{4\gamma^2} K|W|W^2 dt. \tag{4}$$

We assume that the piston-mode motion is uniform and oscillating harmonically inside the moonpool, say $W = W_a \cos(\omega t)$, such that $T = 2\pi/\omega$ is the period and W_a is the amplitude of the piston-mode velocity. By substituting for W and integrating using that $\int_0^T \cos^2 \omega t dt = \pi/\omega$ and $\int_0^{T/4} \frac{1}{4} \cos^3 \omega t dt = \frac{2}{3\omega}$, we obtain

$$\varepsilon = \frac{2KW_a}{3\pi\gamma^2}. \tag{5}$$

The expression (5) for ε involves the pressure drop coefficent K, $\gamma = B_*/L_g$ and the piston-mode water velocity W_a. Having these three parameters at hand, we have a physical-based linear damping coefficient to use in our computations, something which will be of great use in engineering computations. The three parameters are treated in the following.

We discuss K first. This is determined based on the empirical formula given by [4] as

$$K = \left(\frac{1}{C_0(1 - \mathrm{Sn})} - 1 \right)^2, \tag{6}$$

where $C_0 = 0.405 \exp\{-\pi \mathrm{Sn}\} + 0.595$ is the so-called contraction coefficient, and $\mathrm{Sn} = \frac{B_* - L_g}{B_*}$ is the solidity ratio. This expression represents a curve-fit of existing experiments for slatted screens, and thus introduces the empirism of our model for ε.

We next discuss B_*. We propose to estimate this by inverting the formula for the piston mode period in Molin (2001) [6], which gives

$$B_* = 2L_g \exp\left\{ \frac{\pi}{L_g} \left(\frac{T_0^2 g}{4\pi^2} - D \right) - \frac{3}{2} \right\}, \tag{7}$$

where T_0 is the piston mode period and D is the draft.

T_0 is in the present work taken as the peak period in the piston-mode RAO from WAMIT simulations with $\varepsilon = 0$. This represents hardly any additional work, since WAMIT computations are simply repeated, now including ε given by our formulation is to be used with our damping coefficient afterwards.

An alternative way to obtain T_0 is by analytic expressions, if appropriate expressions exist. However, we emphasize that the resonance frequencies, particularly the piston-mode, are different in freely-floating conditions relative to that of forced motion or fixed vessel in waves. Therefore, the analytic formula should not be the solution of the spectral problem, for which several proposed expressions exist, but that of the freely floating problem, for which the solution is much more involved. A pragmatic way is therefore to use the approach in the present work. A good estimate of T_0 is recommended, due to that B_* is quite sensitive to its value, as one can see from inspection of (7).

We last discuss W_a. As in all applications where equivalent linearized damping is applied, one needs to either assume a response amplitude (W_a in our case), or one can determine the response amplitude such that the equation of motion is satisfied, by iteration.

A third option to determine W_a also exists; in the (perhaps rare) case that CFD simulations or model tests exists of the moonpool vessel either forced to heave or freely floating in waves, one can use the obtained amplitude-dependent piston-mode RAO. We refer to the piston-mode RAO as $\mathrm{RAO_g}$, and mean by this the free-surface amplitude averaged over the moonpool. In the case of forced heave, we get

$$W_a = \mathrm{RAO}_g(\omega_0)\omega_0 \eta_{3a} \tag{8}$$

where $\omega_0 = 2\pi/T_0$ is the piston mode frequency and η_{3a} is the forcing amplitude in heave. Using (8) in (5), we get

$$\varepsilon = \frac{2K\, \mathrm{RAO}_g(\omega_0)\omega_0 \eta_{3a}}{3\pi\gamma^2}. \tag{9}$$

Similarly, in case of a freely floating moonpool vessel in waves, we get

$$\varepsilon = \frac{2K\, \mathrm{RAO}_g(\omega_0)\omega_0 \zeta_a}{3\pi\gamma^2}. \tag{10}$$

where ζ_a is the incident wave amplitude, and RAO_g is known from model tests or numerical simulations of the freely floating vessel in waves.

We emphasize that ε is a dimensional parameter with units m/s, which implies that the fluid damping coefficient scales as $\kappa^{0.5}$ when Froude scaling is applied, where κ is the model scale.

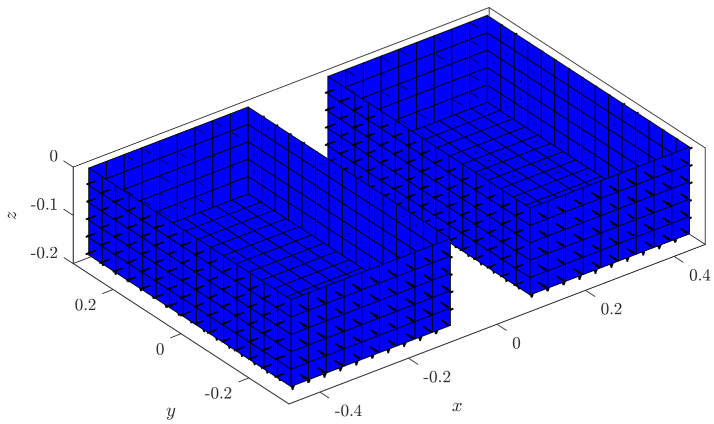

FIGURE 4. MESH USED IN THE WAMIT SIMULATIONS OF CASE 1. THE AXES UNITS ARE IN METERS. THE SURFACE NORMAL VECTORS ARE PRESENTED. WALLS ARE MODELLED AT $y = \pm 0.3$ m.

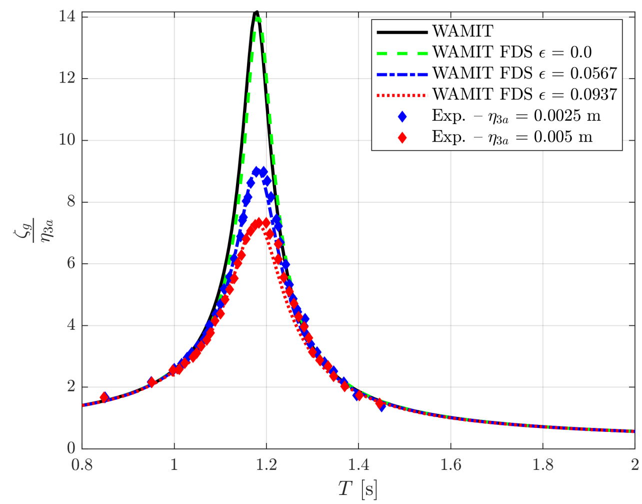

FIGURE 5. AMPLITUDE-DEPENDENT GAP RAOs AT THE MIDDLE OF THE GAP WITH TWO DIFFERENT FORCED HEAVE AMPLITUDES. THE MARKERS INDICATE EXPERIMENTAL RAOs BY KRISTIANSEN AND FALTINSEN (2012) [7], WHEREAS THE SOLID AND DASHED LINES INDICATE GAP RAOs FROM WAMIT SIMULATIONS.

RESULTS AND DISCUSSIONS

We present results from the described model tests and compare our numerical simulations using WAMIT to these, with the intention of showing the validity of our proposed, physical-based damping model (5 - 7). In Case 1 we obtain the damping parameter ε by using (9). In Case 2 we obtain the damping parameter ε by using (10).

Case 1. Forced heave of a 2D moonpool vessel

The mesh applied in the WAMIT simulations is presented in Figure 4. The simulations were performed with two (numerical) channel walls at $y = \pm 0.3$ m, since the model tests were conducted in a two-dimensional setting in a 0.6m wide wave flume.

As explained above, WAMIT was first run without damping, to obtain the piston-mode period T_0. Next, WAMIT was run with damping, applying the formula (9) to obtain ε. The values of the pressure drop coefficient K and the piston-mode natural period T_0 are provided in Table 2. In the table, the two values of ε for the two forcing amplitudes are also provided, both given by (9) with the experimental moonpool $\text{RAO}_g(\omega_0)$ found from Figure 5.

The results are presented in Figure 5. The present WAMIT simulations with the linearized fluid damping coefficients compare very well with the experimental values. This serves as a first validation of our damping model, i.e. the model (5) involving the pressure drop coefficient K given by (6) and γ which involves B_* and implicitly T_0.

Case 2. Freely floating moonpool vessel

TABLE 2. PARAMETERS IN THE DAMPING MODEL FOR CASE 1. ε is computed from (9).

Parameter	Magnitude	Unit
Piston mode period (T_0)	1.18	s
Pressure drop coefficient (K)	15.43	-
ε with $\eta_{3a} = 2.5$ mm	0.0567	m/s
ε with $\eta_{3a} = 5.0$ mm	0.0937	m/s

We next present the results of the second case, which involves a freely floating moonpool vessel in head sea incident waves. Again, WAMIT was first run with $\varepsilon = 0$ to obtain T_0, and next run including damping given by our model.

A coarse mesh of the half-body is presented in Figure 6. The actual mesh used in the computations is significantly refined. Symmetry conditions are applied about the xz-plane at $y = 0$ m.

There are two main differences in Case 2 relative to Case 1: Case 2 is three-dimensional and it involves a freely-floating vessel. To account for that the vessel is freely floating, we apply (10) rather than (9) as used in Case 1.

To account for three-dimensionality we propose to increase the damping coefficient by a factor 2, we call this $\varepsilon_m = 2\varepsilon$. The rationale behind this is that flow separation takes place along all four sides of the moonpool entrance, rather than only along two sides in the two-dimensional case, such that one may expect in the order of twice the pressure drop per unit area of the moonpool inlet. In reality, it is the pressure drop coefficient K that is increased by the factor 2. We acknowledge that the flow at the moonpool entrance is complex, and that this is a rather crude approach.

The values of the pressure drop coefficient K and the piston-mode natural period T_0 are provided in Table 3. The valus of B_* and L_g are those from studying a plane through the moonpool, transverse to the vessel, i.e. beam-wise on the vessel. This is justified by that most of the exterior flow as illustrated in Figure 1 will occur in the plane transverse to the vessel, when the length of the vessel is much larger than the beam.

In Table 3, the two values of $\varepsilon_m = 2\varepsilon$ for the two incident wave steepnesses are also provided, both given by (9) with the experimental moonpool $\text{RAO}_g(\omega_0)$ found from Figure 7.

TABLE 3. PARAMETERS IN THE DAMPING MODEL FOR CASE 2. $\varepsilon_m = 2\varepsilon$. ε is computed from (10).

Parameter	Magnitude	Unit
Piston mode period (T_0)	1.07	s
Pressure drop coefficient (K)	1.89	-
ε_m with $H/\lambda = 1/60$	0.0657	m/s
ε_m with $H/\lambda = 1/30$	0.0957	m/s

Referring to Figure 7, the experimental moonpool responses are, as in Case 1, clearly amplitude-dependent since the quadratic-type damping due to flow separation is dominant. The WAMIT simulations with damping are in fair agreement with the experiments, which suggests that the presently developed damping model provides reasonable estimates of the linearized fluid damping coefficient also in this more realistic three-dimensional case. Although we acknowledge some discrepancies, where the computed piston-mode RAOs are over-predicted by about 20% at piston-mode resonance, the improvement relative to no damping is significant; the simulations not accounting for flow seaparation (damping) over-predicts by an order of magnitude!

The heave and pitch RAOs for the freely floating vessel are presented in Figures 8 and 9, respectively. WAMIT simulations of the vessel without moonpool are also presented for comparison (denoted by MP0 in the legend). The moonpool responses clearly affect the heave and pitch RAOs. The WAMIT simulations without the damping model over-predict also the heave and pitch responses in the vicinity of the piston mode period, and not only the piston-mode itself. WAMIT simulations with damping significantly improve the heave and pitch RAOs compared to those without. Again, the responses are over-predicted by an order of magnitude without damping.

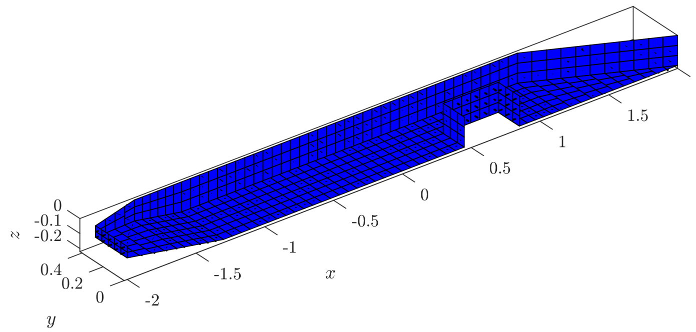

FIGURE 6. EXAMPLE MESH OF THE VESSEL WITH MOONPOOL USED IN THE PRESENT WAMIT SIMULATIONS. ONLY THE HALF-BODY IS MESHED, SINCE SYMMETRY CONDITIONS ABOUT THE xy-PLANE IS APPLIED AT $y = 0$ m.

We conclude that the present methodology to estimate physical-based linearized fluid damping coefficients in linear panel codes, such as WAMIT, may be used as an engineering tool to improve the ship motions as well, in addition to the moonpool responses.

To the best of our knowledge, this represents the first physical-based piston-mode damping model for moonpools that does not rely on any tuning to experimental data for the case at hand.

If experimental data is not available for various reasons, data for a similar vessel may be used in early design or in simulations of marine operations. Othwerwise, our damping model, using iteration or a qualified guess of W_a can be used. The latter is a pragmatic method which is often used in a real, irregular sea state.

In the case that the moonpool has appendages at its inlets, or other structures inside the moonpool, one must expect that our damping model is conservative, i.e. it will provide less damping than in reality, since the pressure drop coefficient K is that of slatted screens with no such irregularities in-between the elements of the screen. A pragmatic (empirical) approach is then to increase the damping coefficient ε according to previous knowledge of how such appendages or internal structures increase the quadratic damping. Relevant studies involving appendages at the moonpool inlet are presented in [9] and [7].

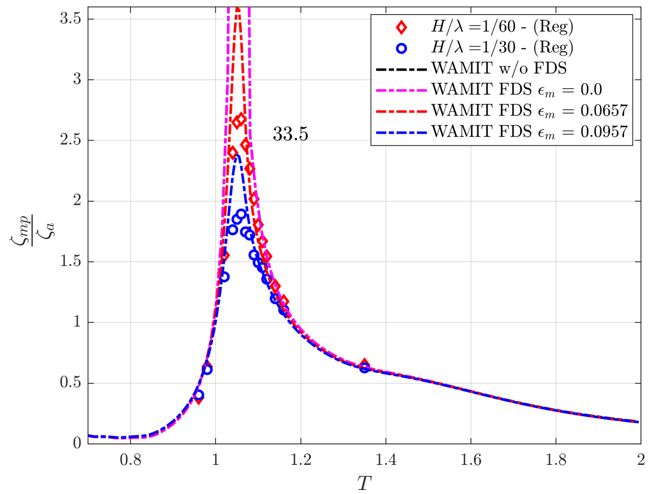

FIGURE 7. MOONPOOL RAOs IN HEAD SEA AT WP1. EXPERIMENTAL RAOs ARE PRESENTED ALONG WITH WAMIT SIMULATIONS WITH AND WITHOUT FLUID DAMPING SURFACES (FDS). THE NUMBER INDICATES THE PEAK VALUE FROM THE WAMIT SIMULATION WITHOUT FDS.

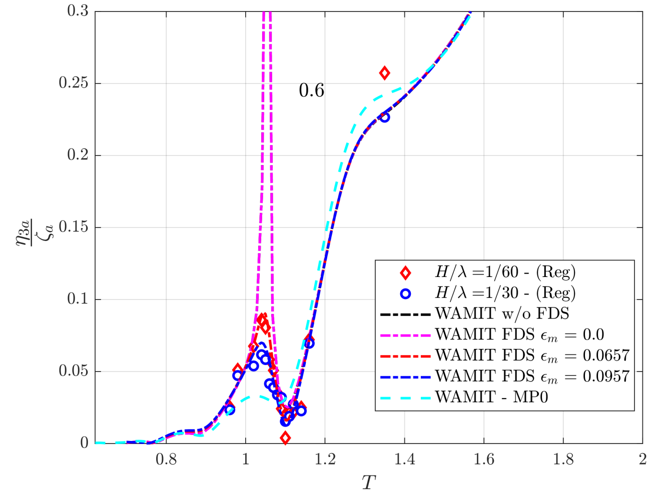

FIGURE 8. HEAVE RAOs IN HEAD SEA FOR CASE 2. EXPERIMENTAL RAOs ARE PRESENTED ALONG WITH WAMIT SIMULATIONS WITH $\varepsilon_m = 0$ and ε_m GIVEN IN TABLE 3. THE NUMBER INDICATES THE PEAK VALUE FROM THE WAMIT SIMULATION WITH $\varepsilon_m = 0$. MP0 ARE WAMIT SIMULATIONS FOR THE VESSEL WITHOUT A MOONPOOL.

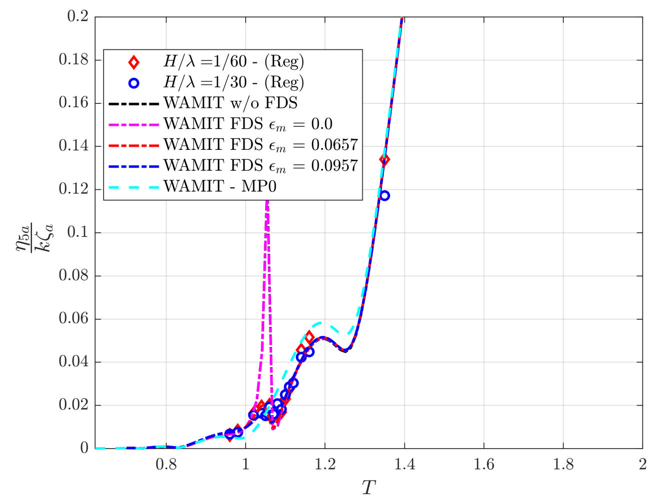

FIGURE 9. SAME AS FIGURE 8, BUT FOR PITCH MOTIONS.

Our damping model is here demonstrated for moonpools. It may be generalized to gap resonance problems such as side-by-side operations when the gap is sufficiently small such that there is limited transverse sloshing inside the gap, by using a damping coefficient ε that varies along the gap.

CONCLUSIONS

We presented a rational, physical-based model for quadratic damping due to flow separation of the piston-mode, with the application of moonpool vessels. The method is based on the novel, semi-empirical method proposed by Faltinsen and Timokha (2015) [4]. Its applicability was demonstrated by two case studies using panel code WAMIT, where a linear damping pressure is added in the free-surface condition inside the moonpool.

The case studies involved a simplified, two-dimensional moonpool vessel forced to heave, as well as a more realistic freely-floating moonpool vessel subjected to head-sea incident waves. By including damping by our proposed model, the moonpool and vessel responses were reproduced within 20% of those obtained in the experiments around piston-mode resonance, while potential flow theory computations over-predicted by an order of magnitude.

Given these positive results, we conclude that the proposed method can be used as an engineering approach to analyse the sea-keeping ability of moonpool vessels, as well as in planning of marine operations involving moonpool vessels.

To the best of our knowledge, this represents the first physical-based piston-mode damping model for moonpools that does not rely on any tuning to experimental data for the case at hand.

The model can be generalized to gap resonance problems, such as side-by-side operations.

ACKNOWLEDGMENT
This research has been funded by the Research Council of Norway, through SFI BLUES, grant number 309281. The authors would like to thank Equinor and SINTEF Ocean, as parts of the numerical work herein was conducted in a joint Equinor/SINTEF Ocean project.

REFERENCES
[1] Kristiansen, T., and Faltinsen, O., 2008. "Application of a vortex tracking method to the piston-like behaviour in a semi-entrained vertical gap". *Applied Ocean Research,* ***30***(1), pp. 1–16.
[2] Watai, R. A., Dinoi, P., Ruggeri, F., Souto-Iglesias, A., and Simos, A. N. "Rankine time-domain method with application to side-by-side gap flow modeling". pp. 69–90.
[3] Ning, D., Su, X., Zhao, M., and Teng, B. "Numerical study of resonance induced by wave action on multiple rectangular boxes with narrow gaps". pp. 92–102.
[4] Faltinsen, O., and Timokha, A., 2015. "On damping of two-dimensional piston-mode sloshing in a rectangular moonpool under forced heave motions". *Journal of Fluid Mechanics,* ***772***.
[5] Ravinthrakumar, S., 2020. "Numerical and experimental studies of resonant flow in moonpools in operational conditions". *PhD thesis*.
[6] Molin, B., 2001. "On the piston and sloshing modes in moonpools". *Journal of Fluid Mechanics,* ***430***, pp. 27–50.
[7] Kristiansen, T., and Faltinsen, O. M., 2012. "Gap resonance analyzed by a new domain-decomposition method combining potential and viscous flow draft". *Applied Ocean Research,* ***34***, pp. 198–208.
[8] Ravinthrakumar, S., Kristiansen, T., Molin, B., and Ommani, B., 2020. "Coupled vessel and moonpool responses in regular and irregular waves". *Applied Ocean Research,* ***96***, p. 102010.
[9] Moradi, N., Zhou, T., and Cheng, L., 2015-07-15. "Effect of inlet configuration on wave resonance in the narrow gap of two fixed bodies in close proximity". pp. 88–102.